The Effects of Coal Mining on Land Use and Land Surface Temperature: A Case Study of Korba District, Chhattisgarh

T. Jaiswal[1] [*], D. Jhariya[1], and N. Kishore[2]

[1] Department of Applied Geology, National Institute of Technology, Raipur 492010, Chhattisgarh, India
[2] Department of Mining Engineering, Indian Institute of Technology, Banaras Hindu University, Varanasi 221005, India

ABSTRACT. Coal is one of the most important mineral which is used as a fuel for generating energy in India, with the increasing urbanization and industrialization, need for more fuel is increasing resulting in extraction of coal in more and more amount, therefore in order to fulfil the demand, mining activities has increased a lot with time, besides the extraction of coal, many other minerals are also being extracted for various purposes as well. Increase in such mining activities are leading to adverse change in air, water and land quality, changes in land use land cover pattern and variation in surface temperature, these continuous changes are therefore, important to be studied in order to assess its impact on the environment for suture sustainability and better management of available resources. The current study has been done for the Korba district with special attention towards the mining areas as major area of the district after agricultural and cultivation land is occupied with mining area and related industries which is on spreading at higher pace since last many years, due to which variation in surface temperature and changes in land use pattern can be seen in its vicinity which is increasing with the time. According to the shifting patterns of land use and land cover, both urban regions and coal mine areas have grown by roughly 35 and 12%, respectively. In the central area of Korba district, the number of mines has risen, and the mining area has expanded over the last thirty years. Through a temporal analysis of the data, the study found that between 2000 and 2021, both the mining zones and adjacent urban areas witnessed increased temperatures. This temperature rise can be linked to the expansion of mining operations and the deforestation that accompanies such activities.

Keywords: LULC, remote sensing, GIS, coal mining, land surface temperature, robust statistics, Korba

1. Introduction

Land use refers to man's activities and the various uses which are carried out on land whereas land covers refer to natural vegetation, water bodies, rock/soil, artificial cover, and others noticed to the land (Prakash and Gupta, 1998). Human activities, especially land use, have changed the physical geographical environment greatly, the direct result of which is the changes of land cover (Simmons et al., 2008). Improper land use practices can adversely affect many natural processes leading to adverse impact on the environment. Rapid growth of mining activities can also be attributed as one of the reasons for decrease and degradation of land. The mining of natural resources is invariably associated with land use and land cover changes (Prakash and Gupta, 1998). Due to the increasing demand for mineral resources driven by industries such as construction and manufacturing, the need for economic development and demand for raw materials driven by urbanization and infrastructure development such activities have also increased.

Mining of coal both surface and subsurface causes enormous damage to the flora, fauna, hydrological relations, and soil biological properties of the systems. Many researchers in their study have discussed these changes due to mining activities and associated changes on land use and temperature. Singh et al. (2017) focused on investigating the land use change dynamics and their impact on surface temperature in the Jharia coalfield region of India using remote sensing and geographical information system (GIS) techniques (Abu et al., 2018). The study found that the land use/land cover changes, particularly due to coal mining activities, had a significant influence on surface temperature. The conversion of vegetation and agricultural lands into mining areas resulted in increased surface temperatures, contributing to the urban heat island effect. Chitade and Katyar (2010) found in heir study that there are significant changes in land use/land cover patterns due to the presence of open-cast coal mines. The study highlights the adverse effects of opencast coal mining on land use and emphasizes the importance of sustainable land management practices to mitigate these impacts. Kayet et al. (2016) revealed in their research that the conversion of forested areas into agricultural and built-up lands had a noticeable impact on surface temperature distribution within the region. The study indicated that areas with increased land use change experienced higher surface temper-

---

[*] Corresponding author. Tel.: +91-9984366669.
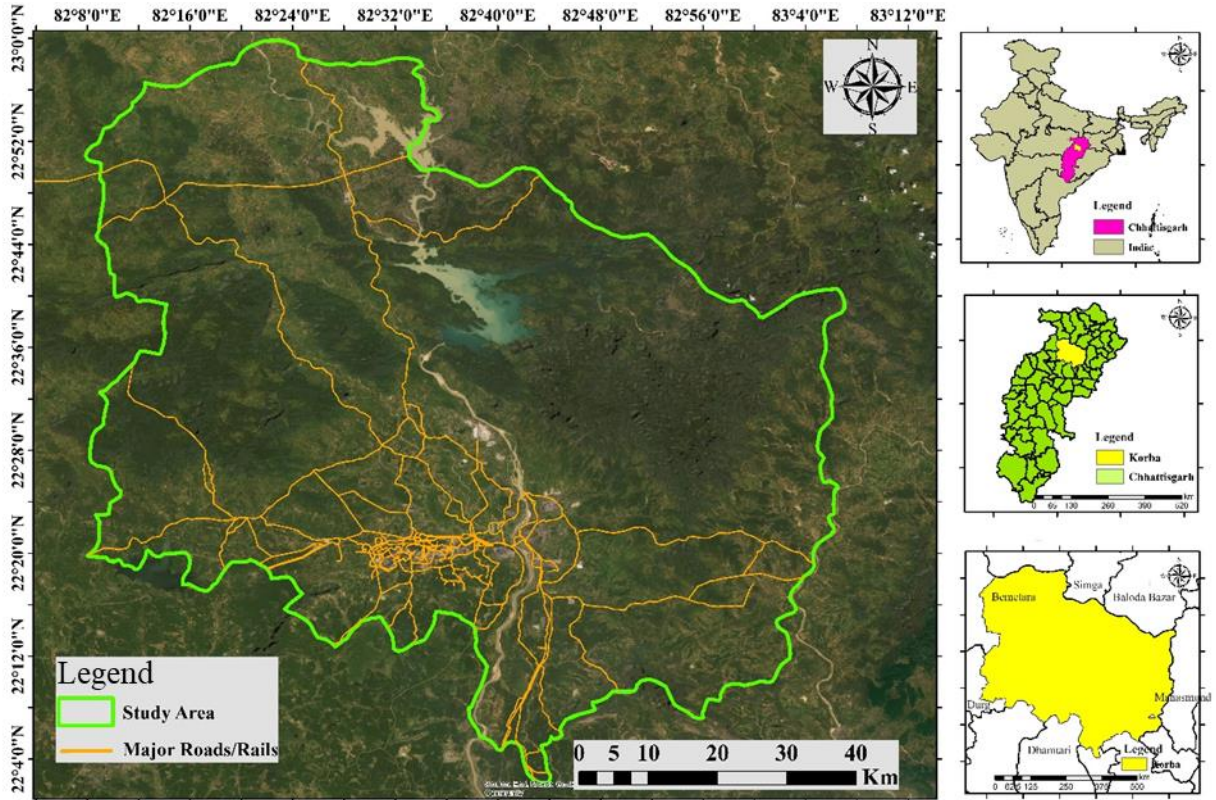*E-mail address:* tanushrijaiswal01@gmail.com (T. Jaiswal).

Figure 1. Location map.

atures compared to areas with intact forest cover. Similarly, Cao et al. (2020) discussed significant spatial variations in land surface temperature associated with mining activities and emphasized the need for effective monitoring and mitigation strategies to minimize the adverse effects of mining on land surface temperature in the area. Das et al. (2021) revealed in their research significant changes in land use/land cover patterns in the area, with urbanization and industrialization leading to the conversion of agricultural and vegetation areas into built-up areas which resulted in increased land surface temperatures, indicating the presence of an urban heat island effect.

The economy of Korba district is dependent on agriculture, but in addition to its significant reliance on agriculture, it is also one of the mineral-rich districts of Chhattisgarh, which is rich in minerals. The district's wealth of mineral resources makes it a significant hub for mines and activities related to mining. Some of the most well-known coal mines in the area include Gevra, Dipika, and Kusmunda, among others; however, in addition to these mines, they also have many more that contain bauxite, dolerite, fireclay, limestone, and granite. There are a total of 65 quarry or mining leases that have been approved in the district of Korba. This includes 15 coal mines, 32 sand mines, six soil mines for the production of bricks, six mines for ordinary stones, five limestone mines, and one fireclay mine (KORBA, 2019). Not only does the process of extracting minerals and other resources from land, which leaves the land deforested and degraded (Firozjaei et al., 2021), have an impact on

the specific areas where these mining activities are being performed, but its clear impact can also be seen in the areas that are in and around the transformed portion of land. Mining areas are identified as LST hotspots due to several factors. Mining activities often involve the removal of vegetation cover and the excavation of land, leading to the exposure of bare soil and rocks. These surfaces have low albedo, meaning they absorb more solar radiation and retain heat, resulting in higher land surface temperatures (LST). Specially in case of coal mining where significant amounts of waste material is generated, such as slag and tailings, which have low thermal conductivity and tend to retain heat. This contributes to elevated LST levels in the vicinity of the coal mines (Saini et al., 2016). The study demonstrated that coal mining activities contributed to increased land surface temperatures in the mining areas compared to non-mining regions.

This is a global problem (Samimi Namin et al., 2011; Katoria et al., 2013; Akter et al., 2021; Firozjaei et al., 2021; Li et al., 2022). Numerous academics are already hard at work studying the negative consequences that these mining activities have on the quality of surface and groundwater, changing patterns of land use, and affecting flora and fauna, among other things (Jaiswal and Jhariya, 2021). The purpose of the current research is to determine the shifts in Land Use and Surface Temperature with the assistance of change detection and to evaluate the effects of changing land use on surface temperature (Basha et al., 2018; Jaiswal and Jhariya, 2020) with specific reference to mining areas and activities related to mining. As a result, thermal
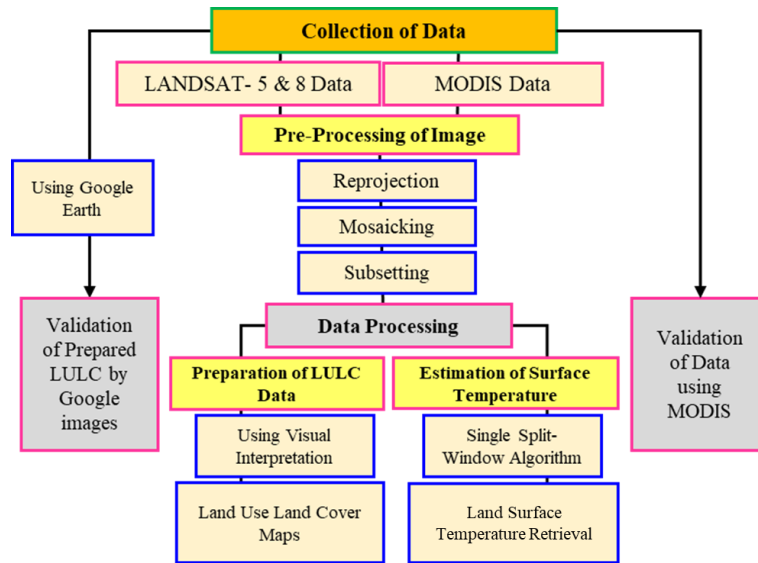
Figure 2. Adopted methodology.

remote sensing data has been used, which is freely available, and after the extraction of datasets and its initial processing, a variety of temperature indices have been It is possible to determine the degree of link between the growing mining area and the rising surface temperature of the district by comparing the statistics for all five years beginning in 2000 and continuing through 2021. As a result, the current study may prove useful in determining its significant effects on vegetation, forest cover, and other aspects that are related to changes in surface temperature.

In this particular research project, the task was carried out by utilizing time-saving and cost-effective approaches such as remote sensing and GIS. Image accuracy is also much improved compared to that of previous historical works because of the substantially higher resolution. The data from Landsat, the Thematic Mapper from Landsat 5, and the Operational Land Imager/Thermal Infrared Sensor from Landsat 8 have been utilized in this study. In addition to this, the temperature data collected by the Moderate Resolution Imaging Spectroradiometer (MODIS) has been utilized to validate the values that were retrieved from Landsat.

2. Study Area

Korba District is located in northern Chhattisgarh, on the bank of the Hasdeo River, which originates in the Sonhat Hills, and is surrounded by the districts of Korea, Surguja, Raigarh, Bilaspur, and Janjgir. The district's southern end is the end of Chhattisgarh's plains; the district's western end is a mix of lowland lands and Maikal hills, while the eastern Korba is governed by the Deopahadi Range (Figure 1).

Korba is notable for its coal mines, such as Gevra, Kusmunda, and Dipika. With prominent power plants like National Thermal Power Corporation Limited (NTPC), Chhattisgarh State Electricity Board (CSEB), and Bharat Aluminium Company (BALCO), the district is known as the power capital of

Chhattisgarh (https://korba.gov.in/).

3. Materials and Methodology

Landsats 5 and 7 Thematic Mapper and (ETM) and Landsat 8 OLI datasets have been used for the years 2000, 2005, 2010, 2015, and 2021 (Table S1). Time-series analyses for Land Use Land Cover (LULC) classification are done using the above data as it is the most extended series of datasets made available by United States Geological Survey (USGS). Further processing for the estimation of LST and change in land-use patterns was performed by the GIS and Image processing software for the same years. Thus, the study includes the methodology given below in Figure 2. for processing the dataset to get the desired output.

3.1. LULC Classification

The technique of visual interpretation has been adopted for the preparation of LULC pattern for the five years from 2000 to 2021 (shown in Figure 3) for the study area. Due to the undulated surface throughout the district area, much of its area is covered with shadow or clouds, which causes a disturbance in the pixel values, resulting in inaccurate results from digital interpretation. Hence, the broad classification has been carried out based on Level 1 classification (Anderson et al., 1976). This classification was performed using the above method for attaining accuracy in classifying the image for both years.

3.2. LST Calculation

Variation in the surface temperature for the Korba district has been estimated using the split-window algorithm (Sobrino et al., 1996, 2003; Mao et al., 2005, 2020; Zhao et al., 2009; Rajeshwari and Mani, 2014; Abdullah and Barua, 2022) by calculating the irradiance, brightness and normalized difference vegetation index (NDVI) values for all the spatial datasets using
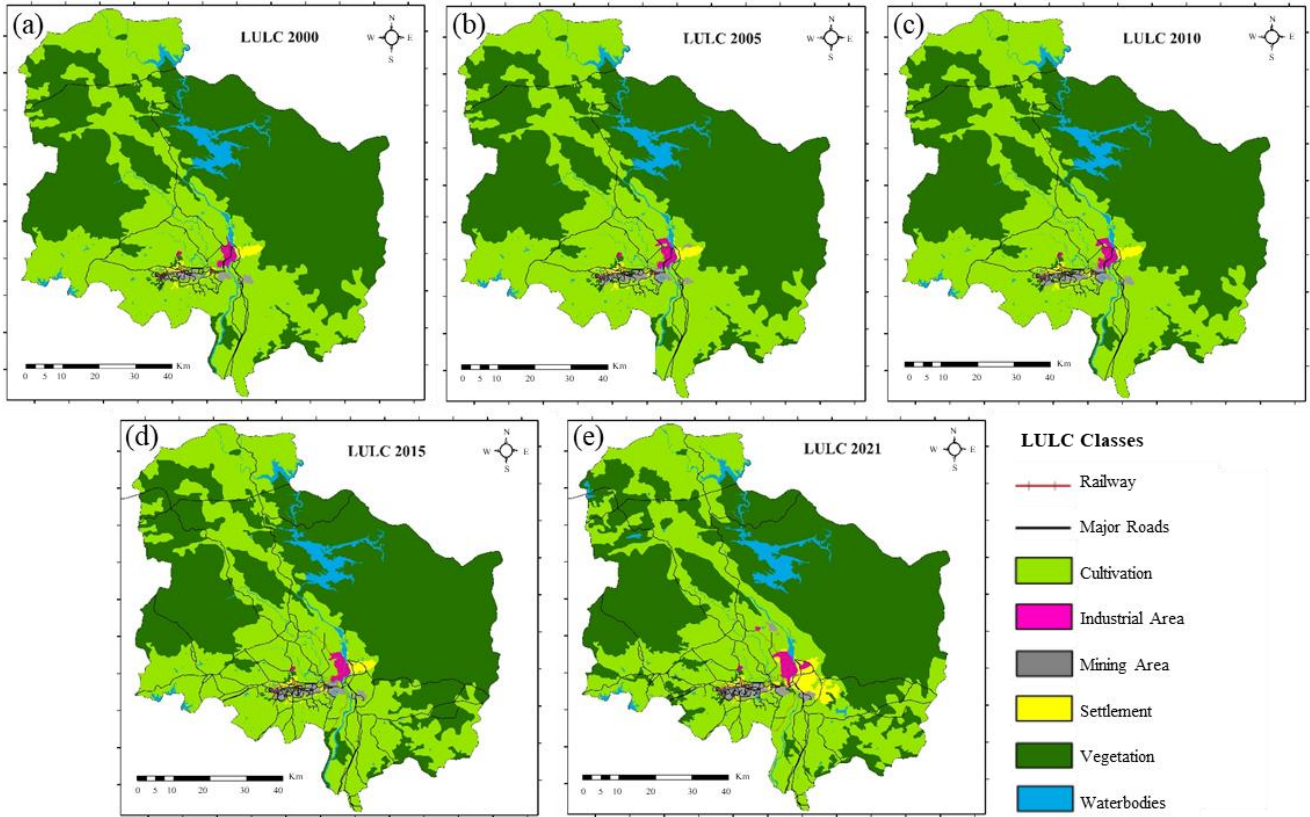
Figure 3. LULC maps for (a) 2000, (b) 2005, (c) 2010, (d) 2015, and (e) 2021.
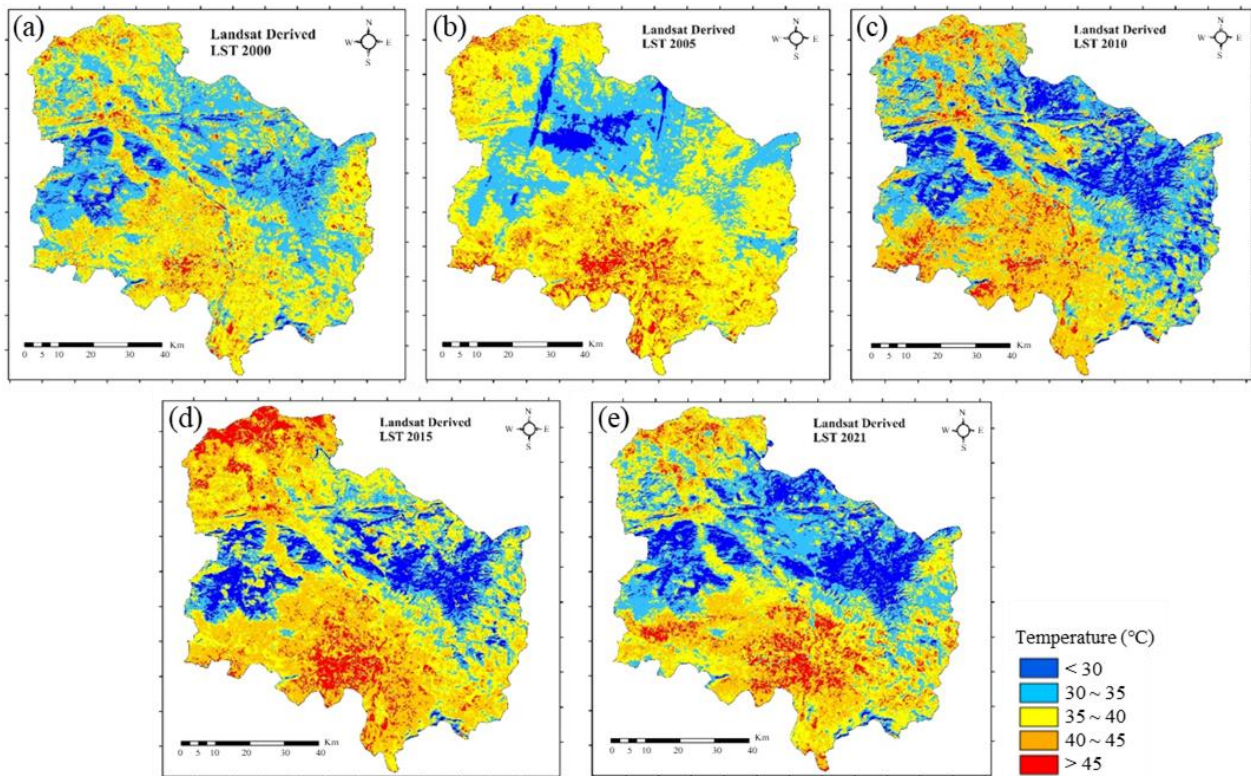
Figure 4. LST maps of Landsat for (a) 2000, (b) 2005, (c) 2010, (d) 2015, and (e) 2021.
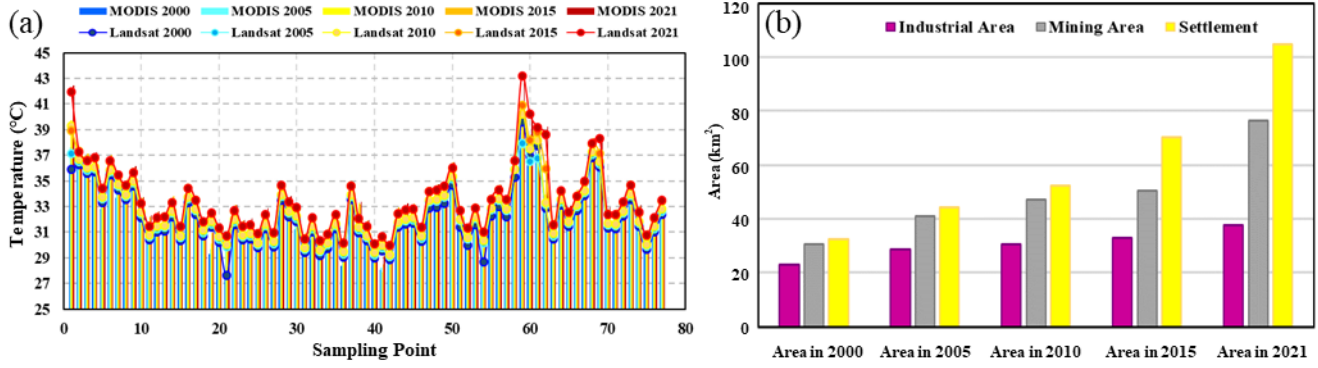
Figure 5. (a) Validation of sampling point temperature from MODIS (2000 ~ 2021) and (b) Change in LULC from 2000 to 2021.

Table 1. Area Occupied (unit: km^2) and their Difference from 2000 to 2021 for LULC Classes

Serial Number	LULC Classes	Area in 2000	Area in 2005	Area in 2010	Area in 2015	Area in 2021	Area Difference (2000 ~ 2021)	% Difference (2000 ~ 2021)
1	Cultivation	2,777.44	2,765.83	2,764.05	2,761.23	2,750.79	−9.91	−0.14976
2	Industrial Area	22.74	28.74	30.43	32.74	37.741	5.04	0.07619
3	Mining Area	30.71	40.89	46.87	50.38	76.38	30.22	0.45681
4	Settlement	32.50	44.29	52.26	70.26	104.78	71.62	1.08276
5	Vegetation	3,536.51	3,525.79	3,513.76	3,495.94	3,443.37	−102.51	−1.54971
6	Waterbody	214.89	209.25	207.39	204.22	201.73	5.54	0.08373

different steps of processing (Figure S1). The whole processing for the retrieval for the years shows enormous variation in temperature for various land-use features (Figure 4) (Jasiwal and Jhariya, 2020, 2021); also expanded urban heat island (UHI) effect has been observed with increasing urbanization and mining area (Mao et al., 2020; Akter et al., 2021; Sankalp et al., 2022). Single split-window algorithm (Sobrino et al., 1996, 2003; Zhao et al., 2009) has been used for estimation from Landsat-5 and 8 images using the step-by-step processing mentioned in detail below.

3.2.1. Spectral Irradiance Calculation

The digital number (DN) values of the TIRS band are converted to top of atmosphere (TOA) radiance using the algorithm by the method of conversion utilizing additive and rescaling factors that are assigned to specific bands stated in the metadata file. This transformation is done so that the radiance value may be calculated using the equation below (Jaiswal and Jhariya, 2020; Akter et al., 2021):

$$L\lambda = ML \times Qcal + AL \tag{1}$$

where $L\lambda$ − the Toa radiance given in Watt/(m^2 × srad × μm); ML − multiplicative rescaling factor for specific band; $Qcal$ − calibrated and quantized standard pixel values of digital number; AL − additive rescaling factor for specific band.

3.2.2. *NDVI* Calculation

The *NDVI* is derived from the infrared (IR) and near-infrared (*NIR*) bands using the algorithm given below, *NDVI* has a range from −1 to +1, and it is used to help with the quantita-

tive assessment of vegetation. Negative values indicate clouds, water, and other non-vegetated, non-reflected surfaces, whereas positive values indicate vegetation and other reflective surfaces:

$$NDVI = (NIR − RED) / (NIR + RED) \tag{2}$$

where NIR − values from *NIR* band; RED – value from red band.

3.2.3. Calculating Fractional Vegetation Cover

A projected percentage of the total study area that is vegetated including various parts of plants, i.e., roots, stems, and leaves is referred to as the fractional vegetation cover (ρ_v), It not only reflects the size of the plant's photosynthetic area and the density of the development of vegetation, but it also shows, to some extent, the growth trend of vegetation which is calculated using the equation mentioned below (Choudhury et al., 1994; Zhang et al., 2019):

$$\rho_v = (NDVI − NDVI_s) / (NDVI_v − NDVI) \tag{3}$$

where ρ_v – fractional vegetation cover; $NDVI_v$ and $NDVI_s$ − *NDVI* values for vegetation and soil respectively.

3.2.4. Calculation of Land Surface Emissivity

The ability of a surface to radiate energy in compared to a black body is measured by its emissivity. The simple relation defines the relationship between reflectivity and emissivity for opaque solids (Li et al., 2013). To convert brightness temperature to kinetic surface temperature, which has been determined using an algorithm, emissivity information is necessary:

$$LSE = \varepsilon_s(1 - FVC) + \varepsilon_v \qquad (4)$$

where ε_v – emissivity from vegetation; ε_s – emissivity from soil; $\rho_v(FVC)$ – fractional vegetation cover.

The average value for the Landsat thermal band is 0.978. The vegetation emissivity ε_v may be estimated as 0.985 (Sobrino et al., 2004):

$$T_s = TB / \{1 + (\lambda \times BT / \rho) \times \log\varepsilon\} \qquad (5)$$

where T_s – the land surface temperature calculated in Kelvin; TB – the brightness temperature in degree; λ – the wavelength of emitted radiance which is 11.5 μm; $\rho = h \times c/\sigma = 1.438 \times 10^{-2}$ mk; h – the plank constant, which is 6.626×10^{-34} J·sec; c – the velocity of light, which is 2.998×10^8 m/sec; σ – the boltzmann constant, which is 1.38×10^{-23} J/K; ε – the surface emissivity:

$$\begin{aligned}LST = {} & TB10 + C1(TB10 - TB11) \\ & + C2(TB10 - TB11)2 + C0 \\ & + (C3 + C4W)(1 - \varepsilon) \\ & + (C5 + C6W)\Delta\varepsilon \end{aligned} \qquad (6)$$

where LST – the land surface temperature; $C0$ to $C6$ – the split-window coefficient values (Sobrino et al., 1996, 2003; Zhao et al., 2009); $TB10$ and $TB11$ – the calculated brightness temperature for band 10 and band 11; ε – the mean LSE of TIR bands; W – the atmospheric water-vapour content; $\Delta\varepsilon$ – the difference in LSE.

3.3. Validation of LST from Landsat Data

MODIS (MOD11A1) LST and Emissivity data which is retrieved daily at the spatial resolution of 1 km (1000 meters) using a split-window algorithm, has been downloaded. MODIS precalculated data product has been used for validating the results for estimated surface temperature from, for this surface temperature product has been taken. It has been observed that almost 90% of results match correctly; for checking this, overall, 77 sampling points (shown in Figure S2) (were taken throughout the district and based on it, a percentage of accuracy has been defined (Figure 5a).

4. Result and Discussion

4.1. Changes in LULC with Special Reference to the Mining Area

LULC maps were classified into five major classes, viz. Vegetation, Cultivation, Waterbodies, Industrial and Settlement, and Mining Area using the remote sensing and GIS platform (Basha et al., 2018). The False-color composite (FCC) results of Landsat 5 and 8 have been analyzed to calculate the changes over the years. The total mining area in 2000 was 30.71 km^2 Showed a continuous spread, and in the year 2021 mining area

increased to 76.38 km^2 (Figure 5b). Also, the total area covered by industrial and settlement areas was 55.24 km^2 in 2000, which rose to 73.03, 82.70, 103.00, and finally 142.52 km^2 in 2005, 2010, 2015, and 2021, respectively, while the cultivation land has declined by 1.91%. Still, a significant change was seen in vegetation cover at about 95.5 km^2 of the total vegetation cover was used for cultivation, mining, industrial or settlement purposes (Table 1). The change in their areas is described in Figure 6. Based on historical reports the unmeritable data, it has been calculated that during 2000 number of mining areas was less with a relatively lesser number of mines, while in the last three decades, the mining area has shown a high rate of increase. It has been observed that many regions regarded as mining areas in 2000 were left untreated after the extraction of minerals from such regions. Area after the extraction of minerals is left barren, and no other activity, like cultivation, etc., can be performed in those areas due to soil infertility.

4.2. Change in Retrieved LST Values

LST values for all the years were calculated using the mono-window algorithm (Sobrino et al., 1996, 2003; Zhao et al., 2009) and based on obtained output from the developed maps (Figure S3), it can be observed that reflectance from urban, mining, industrial and open land has higher values in comparison to natural landscapes which means lower reflectance from cultivated, vegetative land and waterbody resulting in lower LST values in contrast to the built-up or barren land with higher reflectance value, Therefore, by the above output, it can be illustrated that there is variation in surface temperature of place depending on its LULC type which means the transformation of land use from cultivated, vegetation or barren land into a human-influenced feature like urban, industrial or mining area is giving rise to increased temperature in and around the place.

4.3. Mining Impacts on LST

For analyzing the impacts of mining activities on LST over time, the total area was divided into a grid of 9×9 km^2. The midpoint for each column was taken to assess the temperature overall 77 such points were taken (shown in Figure S2). It has been observed that the areas, explicitly mining and industrial, have much higher temperatures, and the pixels with higher temperature values are spreading in the pattern of increasing mining areas (Figure S4). Moreover, it has been seen that the areas with no or lesser transformation show significantly less temperature variation. In contrast, the UHI effect highly affected the mining and nearby developing regions. Specifically, the central part of the district, which has the majority of coal fields, mainly seemed to be affected by the increasing temperature (shown in Figure 7).

Thus, a significant difference in LULC pattern and LST in the central part of the district can be seen in the last two decades, i.e., 2000 ~ 2021. A direct relationship can be established between LST and LULC as there was a maximum temperature in the vicinity of mining areas, decreasing with the distance away more transformation has been done in urban and mining areas (Figure S5), resulting in higher temperatures for such sites. This variation in surface temperature with the changing land cover
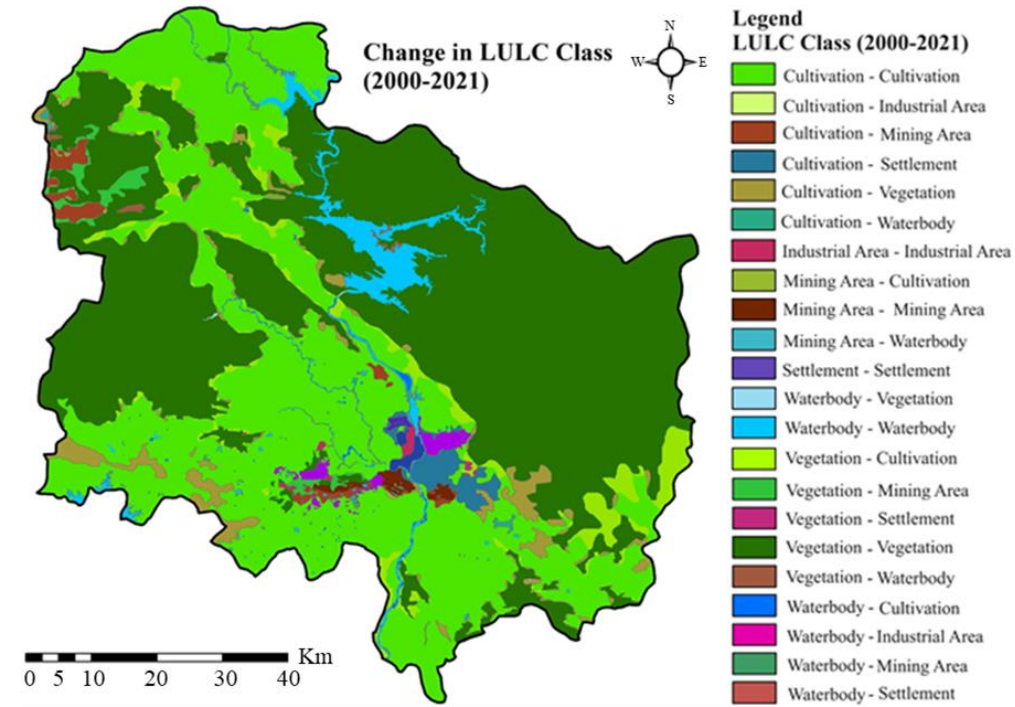
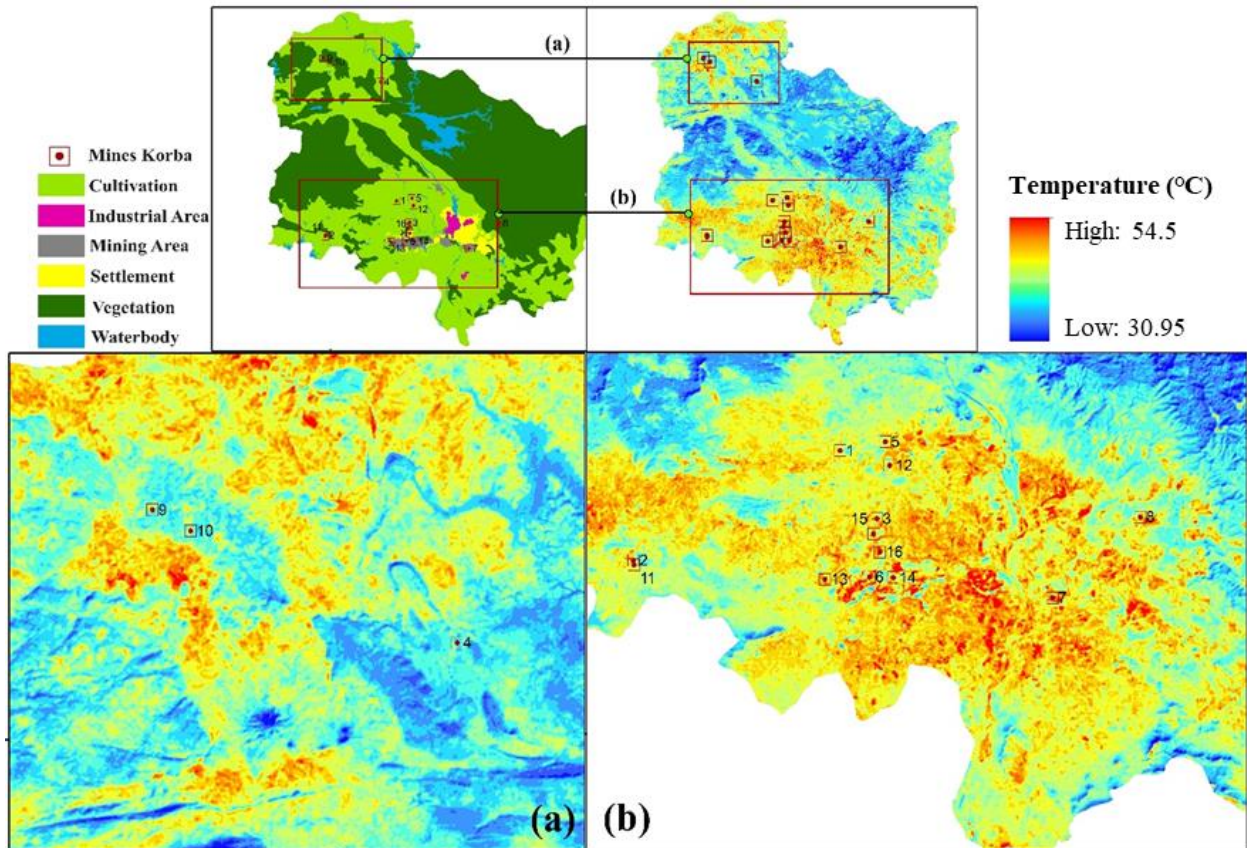**Figure 6.** The year-wise difference in % area from 2000 to 2021.

Figure 7. High temperature in the vicinity of the mining area at two locations (a) and (b) in Korba district.
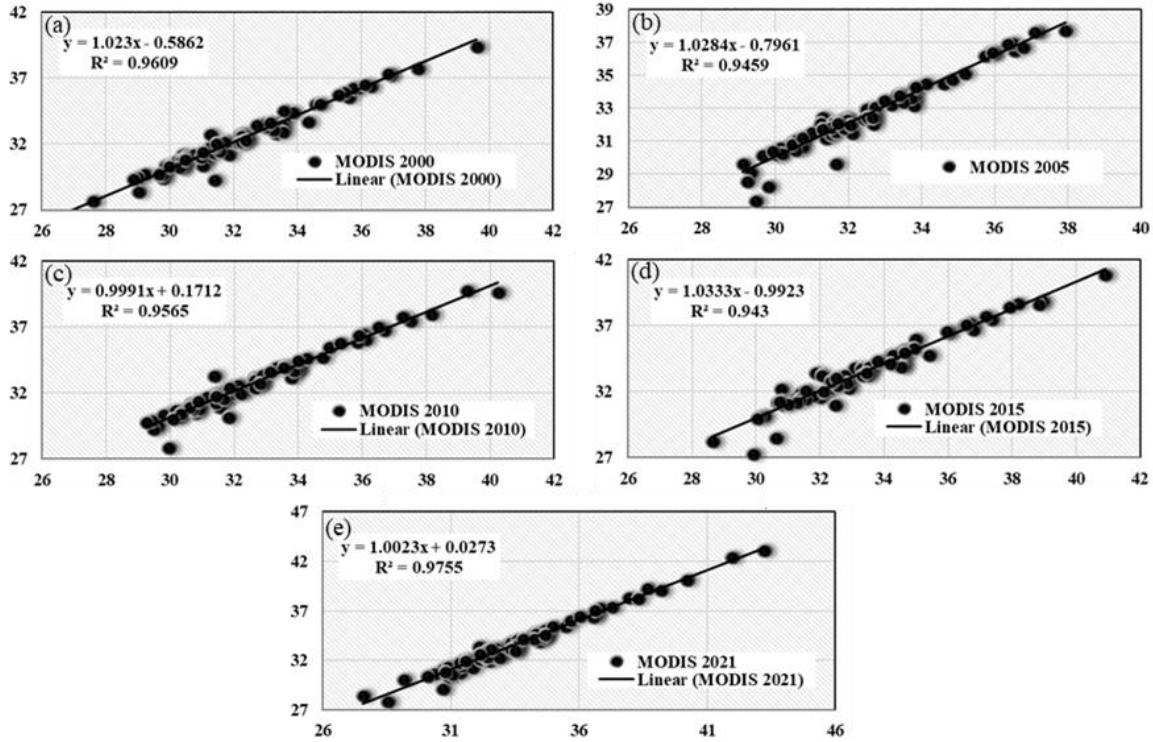
Figure 8. Cross-validation of Landsat derived LST with MODIS for (a) 2000, (b) 2005, (c) 2010, (d) 2015, and (e) 2021.

Table 2. Classification of Threshold Temperature Values

Threshold for Temperature	$T \leq -1.5\ sd$	$-1.5 < T \leq -1\ sd$	$-1 < T \leq -0.5\ sd$	$-0.5 < T \leq 0.5\ sd$	$0.5 < T \leq 1\ sd$	$1 < T \leq 1.5\ sd$	$T > 1.5\ sd$
Classification for Temperature	Extremely Low	Very Low	Low	Moderate	High	Very High	Extremely High

Table 3. Statistical Representation of Classified Area (in Percent) for Surface Temperature

Year	High Temperature ($> 0.5\ sd$)	Moderate Temperature ($-0.5 \sim 0.5\ sd$)	Low Temperature ($< -0.5\ sd$)
2000	30.729	26.147	43.125
2005	32.875	31.625	35.500
2010	35.639	39.860	24.501
2015	30.729	26.147	43.125
2021	32.875	31.625	35.500

shows a direct correlation between increasing temperature with expanded mining and urban sprawl (Table S2).

Cross-validation of retrieved mean LST values with same spatial reference was used for the validation step with MODIS-derived LST values and it was found that there was approx. average difference of ±2 °C at most of the places while at few places, the difference was more which may be due to the difference in scale of the two datasets (Jaiswal and Jhariya, 2023). The best graphical representation method for contrasting two quantitative variables is a scatterplot with linear regression where R^2 indicates a model's fit. The R^2 coefficient of determination measures how closely regression predictions match real data points. The value of R^2 from 0.7 and above is considered to be a good data match. This method is used by different researchers

for comparing and correlation of their data (Bosilovich 2006) for the comparison of temperature values derived from Landsat data with MODIS-derived data (Duan et al., 2017). Obtained results show the high value of R^2 ranging between 0.94 to 0.97 (Figure 8).

4.4. Statistical Analysis of Estimated Surface Temperature

Minimum, maximum, mean, and standard deviation values for five years were calculated from retrieved surface temperature images and statistically analyzed the surface temperature distribution (Table S3) over the area. Robust statistics is a group of techniques used for estimating the parameters of a parametric model when working with ideal assumption-based deviations (Hampel et al., 1986; Zhang et al., 2007) has been used for the

classification of surface temperature formula used for calculating the threshold value is given below (Yang and Liu, 2020):

$$T = A \pm x \times sd \qquad (7)$$

where T – the threshold value for temperature; A – the average calculated surface temperature; x – the multiple of variance (0.5, 1, and 1.5), and sd – the variance of surface temperature.

By multiplying x with the standard deviation (sd) and adding or subtracting the result from the mean (A), you can establish a threshold range or boundary for further analysis or classification of estimated temperature values. The $\pm$ sign indicates that you can choose to add or subtract the product of x and sd, depending on the desired threshold value for temperature.

As per the calculated threshold values, the area's temperature has been divided into seven grades, i.e., shallow, deficient, low and moderated temperature, and so on; tabular distribution of threshold value of temperature according to the grades is given in Table 2.

The area (in pixels) that corresponds to each classified quality has been computed for all five years, from 2000 to 2021, using temperature grades as the basis. Statistics are generated, which show that a place with a temperature that is higher than 0.5 times the standard deviation (sd) is classified as belonging to the High-temperature region, whereas an area that has a temperature that is lower than -0.5 sd is classified as belonging to the Low-temperature region, and those areas that fall within the variance value range of $+0.5$ to -0.5 are regarded as belonging to the Moderate-temperature region Table 3 shows the statistical presentation of % area covered by each class.

5. Conclusions

In the state of Chhattisgarh, the district of Korba is recognized as the power capital of the state. It is one of the significant districts that contributes to mining and other related activities, which in turn leads to rapid urbanization and industrialization, which in turn results in negative effects that have an impact on the environment. The current study was carried out with the purpose of analysing these unfavourable effects of mining, with a specific emphasis on the coal mines in the area. This is due to the fact that the area contains the maximum number of coal mines in the area, which is the reason why a variety of thermal plants were also established nearby. These plants are giving their massive contribution toward polluting the ecosystem and increasing temperature, and the study was carried out with the help of freely available remotely sensed data and advanced GIS techniques. During the past three decades, the Korba district has been analysed with photos from five different phases. According to the findings, between the years 2000 and 2021 continuous increase in the mining and neighbouring urban areas with greater temperatures as well as the other locations with lower temperature data are decreasing annually. Even Nevertheless, the frequency of temperature rises is more likely to occur in metropolitan areas as compared to non-urban locations. The study highlights the use of remote sensing and GIS technology for evaluating the impacts of mining activities, specifi-

cally by utilizing satellite-derived thermal data. This technology has proven to be highly effective in monitoring and assessing the changes in land surface temperature associated with mining activities. By analysing thermal data from satellites, researchers can detect thermal anomalies and identify areas affected by mining operations. This information is valuable for understanding the extent and spatial distribution of mining impacts on land cover and surface temperature.

Furthermore, the study suggests that combining remote sensing and GIS data with other sources of information, such as ground truth verification and data on surface and groundwater, can enhance the accuracy and comprehensiveness of the analysis. Ground truth verification involves on-site measurements and observations to validate and refine the remote sensing data. Integrating such additional data allows researchers to investigate the broader impacts of land use changes, including their effects on water resources, ecosystems, and other relevant parameters.

Also, some simple mitigating measures can be implemented to overcome the increasing temperature in the vicinity of mining areas, which includes:

- Planting trees and creating green belts around the mining areas can help regulate temperatures by providing shade and reducing the heat island effect.
- Also mined areas which are left untreated can be restored as water bodies and wetlands can help in cooling the surrounding environment through evaporative cooling and creating microclimates.
- Heat-Resistant Infrastructure with materials and techniques that are resistant to heat and can minimize heat transfer can be introduced in order to mitigate temperature rise in the vicinity.

In summary, the research highlights the capacity of remote sensing and GIS technology, specifically satellite-based thermal data, to monitor and assess the effects of mining on land use and land surface temperature. The integration of these technologies with additional data sources and verification methods allows for more precise and holistic findings, leading to an improved comprehension of the environmental impact of human activities. By leveraging these technologies and adopting simple measures, it becomes possible to promote sustainable practices and better manage the environment.

References

Abdullah, S. and Barua, D. (2022). Modeling land surface temperature with a Mono-Window algorithm to estimate urban heat island intensity in an expanding urban area. *Environmental Processes*, 9, 14. https://doi.org/10.1007/s40710-021-00554-8

Abu, E.K., Lacroix, P., Sivalingam, P., Ray, N., Giuliani, G., Mulaji, C.K., Otamonga, J.P., Mpiana, P.T., Slaveykova, V.I. and Poté, J. (2018). High contamination in the areas surrounding abandoned mines and mining activities: An impact assessment of the Dilla, Luilu, and Mpingiri Rivers, the Democratic Republic of the Congo. *Chemosphere*, 191, 1008-1020. https://doi.org/10.1016/j.chemosphere.2017.10.052

Akter, T., Gazi, M.Y. and Mia, M.B. (2021). Assessment of land cover dynamics, land surface temperature, and heat island growth in north-

western Bangladesh using satellite imagery. *Environmental Processes*, 8, 661-690. https://doi.org/10.1007/s40710-020-00491-y

Anderson, J.R., Hardy, E.E., Roach, J.T. and Witmer, R.E. (1976). *A Land Use and Land Cover Classification System for Use with Remote Sensor Data*. US Government Printing Office, 964.

Basha, U.I., Suresh, U., Raju, G.S., Rajasekhar, M., Veeraswamy, G. and Balaji, E. (2018). Landuse and landcover analysis using remote sensing and GIS: A case study in somavathi river, Anantapur District, Andhra Pradesh, India. *Nature Environment and Pollution Technology*, 17(3), 1029-1033.

Cao, J.S., Deng, Z.Y., Li, W. and Hu, Y.D. (2020). Remote sensing inversion and spatial variation of land surface temperature over mining areas of Jixi, Heilongjiang, China. *PeerJ*, 8, e10257. https://doi.org/10.7717/peerj.10257

Chitade, A.Z. and Katyar, S.K. (2010). Impact analysis of open cast coal mines on land use/land cover using remote sensing and GIS technique: A case study. *International Journal of Engineering Science and Technology*, 2(12), 7171-7176.

Choudhury, B.J, Ahmed, N.U, Idso, S.B, Reginato, R.J. and Daughtry, C.S. (1994). Relations between evaporation coefficients and vegetation indices studied by model simulations. *Remote sensing of environment*, 50(1), 1-17. https://doi.org/10.1016/0034-4257(94)90090-6

Das, N., Mondal, P., Sutradhar, S. and Ghosh, R. (2021). Assessment of variation of land use/land cover and its impact on land surface temperature of Asansol subdivision. *The Egyptian Journal of Remote Sensing and Space Science*, 24(1), 131-149. https://doi.org/10.1016/j.ejrs.2020.05.001

Firozjaei, M.K., Sedighi, A., Firozjaei, H.K., Kiavarz, M., Homaee, M., Arsanjani, J.J., Makki, M., Naimi, B. and Alavipanah, S.K. (2021). A remote sensing-based approach is a historical and future impact assessment of mining activities on surface biophysical characteristics change. *Ecological Indicators*, 122, 107264. https://doi.org/10.1016/j.ecolind.2020.107264

Hampel, F.R., Ronchetti, E.M., Rousseeuw, P.J. and Stahel, W.A. (1986). *Robust Statistics: The Approach Based on Influence Functions*, John Wiley & Sons, pp 196. ISBN: 0471735779

Jaiswal, T. and Jhariya, D.C. (2020). Impacts of land use land cover change on surface temperature and groundwater fluctuation in Raipur District. *Journal of the Geological Society of India*, 95, 393-402. https://doi.org/10.1007/s12594-020-1448-6

Jaiswal, T. and Jhariya, D.C. (2021). Monitoring the Land Surface and water bodies temperature and its impact on surface water turbidity in Raipur, Chhattisgarh, India. *IOP Conference Series: Earth and Environmental Science*, 597, 012008. https://doi.org/10.1088/1755-1315/597/1/012008

Jaiswal, T., Jhariya, D. and Singh, S. (2023). Spatio-temporal analysis of changes occurring in land use and its impact on land surface temperature. *Environmental Science and Pollution Research*, 1-20. https://doi.org/10.1007/s11356-023-26442-2

Katoria, D., Sehgal, D. and Kumar, S. (2013). Environment impact assessment of coal mining. *International Journal of Environmental Engineering and Management*, 4(3), 245-250.

Kayet, N., Pathak, K., Chakraborty, A. and Sahoo, S. (2016). Spatial impact of land use/land cover change on surface temperature distribution in Saranda Forest, Jharkhand. *Modeling Earth Systems and Environment*, 2, 1-10, https://doi.org/10.1007/s40808-016-0159-x

KORBA (2019). District survey report. https://korba.gov.in/documents/ (accessed September 30, 2019).

Li, X., Zhou, Y. and Wang, F. (2022). Advanced information mining from ocean remote sensing imagery with deep learning. *Journal of Remote Sensing*, 2022, 9849645. https://doi.org/10.34133/2022/9849645

Li, Z.L., Wu, H., Wang, N., Qiu, S., Sobrino, J.A., Wan, Z.M., Tang, B.H. and Yan, G.J. (2013). Land surface emissivity retrieval from satellite data. *International Journal of Remote Sensing*, 34(9-10), 3084-3127. https://doi.org/10.1080/01431161.2012.716540

Mao, K., Qin, Z., Shi, J. and Gong, P. (2005) A practical split-window algorithm for retrieving land-surface temperature from MODIS data. *International Journal of Remote Sensing*, 26(15), 3181-3204. https://doi.org/10.1080/01431160500044713

Mao, C.C., Xie, M.M. and Fu, M.C. (2020). Thermal response to patch characteristics and configurations of industrial and mining land in a Chinese mining city. *Ecological Indicators*, 112, 106075. https://doi.org/10.1016/j.ecolind.2020.106075

Prakash, A. and Gupta, R.P. (1998). Land-use mapping and change detection in a coal mining area – A case study in the Jharia coalfield. India. *International Journal of Remote Sensing*, 19(3), 391-410. https://doi.org/10.1080/014311698216053

Rajeshwari, A .and Mani, N.D. (2014). Estimation of the land surface temperature of Dindigul district using Landsat 8 data. *International journal of Research in Engineering and Technology*, 3(5) 122-126.

Saini, V., Arora, M.K. and Gupta, R.P. (2016). Relationship between surface temperature and SAVI using Landsat data in a coal mining area in India. *In Land Surface and Cryosphere Remote Sensing III*. 9877, 114-119. https://doi.org/10.1117/12.2228094

Samimi Namin, F., Shahriar, K. and Bascetin, A. (2011). Environmental impact assessment of mining activities. A new approach for mining methods selection. *Gospodarka Surowcami Mineralnymi*, 27, 113-143.

Sankalp, S. and Sahoo, S.N. (2022). Grey Relational Modelling of Land Surface Temperature (LST) for Ranking Indian Urban Cities. *Environmental Processes*. 9(2), 32. https://doi.org/10.1007/s40710-022-00588-6

Simmons, J.A., Currie, W.S., Eshleman, K.N., Kuers, K., Monteleone, S., Negley, T.L., Pohlad, B.R. and Thomas, C. L. (2008). Forest to reclaimed mine land use change leads to altered ecosystem structure and function. *Ecological Applications*, 18(1), 104-118. https://doi.org/10.1890/07-1117.1

Singh, P., Kikon, N. and Verma, P. (2017). Impact of land use change and urbanization on urban heat island in Lucknow city, Central India. A remote sensing based estimate. *Sustainable cities and society*. 32, 100-114. https://doi.org/10.1016/j.scs.2017.02.018

Sobrino, J.A., Li, Z.L., Stoll., M.P. and Becker, F. (1996). Multi-channel and multi-angle algorithms for estimating sea and land surface temperature with ATSR. *International Journal of Remote Sensing*, 17(11), 2089-2114, https://doi.org/10.1080/01431169608948760

Sobrino, J.A., El Kharraz, J. and Li, Z.L. (2003). Surface temperature and wavaporpour retrievals from MODIS data. *International Journal of Remote Sensing*, 24(24), 5161-5182. https://doi.org/10.1080/0143116031000102502

Yang, Z. and Liu, N.N. (2020). Inversion and Analysis of Land Surface Temperature based on Landsat – A case study of BeiBei District in Chongqing. *2020 2nd International Conference on Civil Architecture and Energy Science (CAES 2020)*, 165, 03006. https://doi.org/10.1051/e3sconf/202016503006

Zhang, J., Wang, Y. and Wang, Z. (2007). Change analysis of land surface temperature based on robust statistics in the estuarine area of Pearl River (China) from 1990 to 2000 by Landsat TM/ETM+ data. *International Journal of Remote Sensing*, 28(10), 2383-2390. https://doi.org/10.1080/01431160701236811

Zhang, S.Q., Chen, H., Fu, Y., Niu, H.H., Yang, Y. and Zhang, B.X. (2019). Fractional vegetation cover estimation of different vegetation types in the Qaidam Basin. *Sustainability*, 11(3), 864. https://doi.org/10.3390/su11030864

Zhao, S.H., Qin, Q.M., Yang, Y.H., Xiong, Y.J. and Qiu, G.Y. (2009). Comparison of two split-window methods for retrieving land surface temperature from MODIS data. *Journal of Earth System Science*, 118, 345. https://doi.org/10.1007/s12040-009-0027-4